Environmental Science
Water Research & Technology

ROYAL SOCIETY OF CHEMISTRY

PAPER

Cite this: *Environ. Sci.: Water Res. Technol.*, 2023, **9**, 363

Emerging investigator series: microplastic-based leachate formation under UV irradiation: the extent, characteristics, and mechanisms†

Ashton Collins,[a] Mohamed Ateia,[b] Kartik Bhagat,[c] Tsutomu Ohno,[d] François Perreault [c] and Onur Apul *[a]

Received 4th June 2022,
Accepted 8th December 2022

DOI: 10.1039/d2ew00423b

rsc.li/es-water

Microplastics in the aquatic system are among the many inevitable consequences of plastic pollution, which has cascading environmental and public health impacts. Our study aimed at analyzing surface interactions and leachate production of six microplastics under ultraviolet (UV) irradiation. Leachate production was analyzed for the dissolved organic content (DOC), UV_{254}, and fluorescence through excitation emission (EEM) to determine the kinetics and mechanisms involved in the release of organic matter by UV irradiation. The results suggested there was a clear trend of organic matter being released from the surface of the six microplastics caused by UV irradiation based on DOC, UV_{254} absorbance, and EEM intensity increasing with time. Polystyrene had the greatest and fastest increase in DOC concentrations, followed by the resin coated polystyrene. Experiments conducted at different temperatures indicated the endothermic nature of these leaching mechanisms. The differences in leachate formation for different polymers were attributed to their chemical makeup and their potency to interact with UV. The aged microplastic samples were analyzed by Fourier-transform infrared spectroscopy (FT-IR), Raman, and X-ray photoelectron spectroscopy (XPS), to determine the surface changes with respect to leachate formation. Results indicated that all microplastics had increasing carbonyl indices when aged by UV with polystyrene being the greatest. These findings affirm that the leachate formation is an interfacial interaction and could be a significant source of organic compound influx to natural waters due to the extremely abundant occurrence of microplastics and their large surface areas.

Water impact

Microplastic pollution of the aquatic system has multifaceted and cascading public health implications. This study aimed at unraveling the leachate dissolution mechanisms from microplastics. The work indicated that there is a clear pattern of dissolved organic matter release from microplastics into water depending on the microplastic type, UV intensity, water temperature, and stirring regime.

1. Introduction

Plastic production rate has increased from 2 to 380 Mt per year over the past 70–80 years due to their inexpensive production and broad use.[1] This had led to approximately five trillion pieces of plastics in the world's oceans.[2] The increasing mass of plastic debris in aquatic systems causes the formation of smaller plastic particles, which is attributed to the physicochemical and biological weathering of plastics in the natural environment *via* ultraviolet (UV) irradiation, hydrolysis, biodegradation, physical abrasion, and thermal degradation.[3,4] These smaller plastic particles (*i.e.*, microplastics, MPs) form a new anthropogenic domain dubbed "the microplastisphere".[5,6] Due to the excessively large surface area of the microplastisphere it is essential to understand the physicochemical processes that occur at the interface of microplastics in aquatic environments.[7,8] The UV driven degradation of microplastics causes their surface oxidation and formation of organic leachate in water, a mixture of dissolved organic matter (DOM).[9] Leachate

[a] *Department of Civil and Environmental Engineering, University of Maine, Orono, ME 04473, USA. E-mail: onur.apul@maine.edu*
[b] *United States Environmental Protection Agency, Center for Environmental Solution & Emergency Response, Cincinnati, OH, USA*
[c] *School of Sustainable Engineering and the Built Environment, Arizona State University, Tempe, AZ, 85287, USA*
[d] *School of Food and Agriculture, University of Maine, Orono, ME 04473, USA*

† Electronic supplementary information (ESI) available: The supporting information section contains photographs of the microplastics used, a schematic of the experimental set-up, a summary of DOC data for each polymer type, and the raw Raman data. See DOI: **https://doi.org/10.1039/d2ew00423b**

formation may have implications on water quality because conventional water treatment plants are not purposefully designed to remove microplastic leachate. In addition, DOM released from the microplastisphere may have direct ecological and health implications or indirect impacts such as disinfection byproduct formation.[10]

There are a handful of studies investigating how MPs break down in the environment by using UV irradiation as simulated sunlight and by concurrently monitoring the changes in surface characteristics and leachate formation for various polymer types.[11,12] Polystyrene (PS) is the most common polymer chosen in these studies, followed by polypropylene (PP), polyvinyl chloride (PVC), and polyethylene (PE).[7] Numerous studies have shown the importance of UV irradiation as a direct factor in the breakdown of polymers in the aquatic environment where either idealized or realistic MP samples are aged with a varying amount of UV intensity and exposure time. UV irradiation time has ranged from a few hours to months to understand the varying effects of high-intensity, short-term irradiation as well as low-intensity, long-term irradiation on MPs.[13–15] Varying wavelengths within the UV spectrum have been chosen from UV-A (315–400 nm), UV-B (280–315 nm), and UV-C (100–280 nm). UV-A is used for simulated sunlight most frequently because 95% of UV light from the Sun is comprised of UV-A wavelengths, where ozone absorbs the majority of UV-B and UV-C.[16] In most environments where oxygen is present, surface of the polymer will oxidize *via* photooxidation where UV light or UV-based oxidants interact with the chemical bonds of polymers.[17–20] Photooxidation of MP surfaces could alter the fate of MPs and their overall interactions with the environment in natural waters.

A study by Wang *et al.* (2020) investigated the surface oxidation of PVC using Fourier-transform infrared spectroscopy (FT-IR), and Fourier-transform infrared imaging spectroscopy imaging (FT-IRIS) for surface degradation after 2 d of 40 mW cm^{-2} UV-A irradiance and demonstrated the importance of particle size.[21] Studies by Lee *et al.* (2020a, b)[9,23] showed an analysis of PS, PVC, PE and PP-based leachate concentrations and surface degradation from 14 d of aging and compared against dark conditions. Xenon lamps at UV-A range were used in an artificial freshwater environment applying 4 mW cm^{-2} of solar irradiance.[23] The study found that PP leached 42.1 mg L^{-1} (42.1 mg DOC g MP^{-1}) and PE leached 22.8 mg L^{-1} (22.8 mg DOC g MP^{-1}) after the 14 d of aging period in 125 mL cylindrical quartz tubes with 50 mg MP and 50 mL water. Release of dissolved organic carbon (DOC) was significantly higher under irradiation conditions than in the dark conditions.[23] Similarly, PS leached 15.2 mg L^{-1} and PVC leached 2.24 mg L^{-1} after the 14 d aging period in quartz containers; however, the irradiation power and MP content of the test was not noted.[9] Other studies using UV-A have looked at adsorption potential for aged MPs, and degradation in different aquatic environments, but these studies did not combine DOC leaching and surface analysis.[18–22] Despite these recent studies, there is still a clear need to advance the fundamental understanding of DOM formation and surface oxidation under UV irradiation *via* side-by-side analysis of common polymers.

This study experimentally tested interaction of six polymer types side-by-side under UV-A irradiation. Specifically, three modes of liquid and three modes of solid phase analysis were conducted to present additional evidence of the direct link between the mechanisms creating the oxidation of polymer's surface releasing organic matter into the surrounding environment. The four specific objectives of this study are to: (1) determine the effect of polymer types and UV aging conditions on DOM formation; (2) conduct surface characterization using FT-IR, Raman spectroscopy (RAMAN), and X-ray photoelectron spectroscopy (XPS) to understand the changes in MP surface; (3) relate the changes in surface characteristics and the amount of DOM leached and; (4) reveal the physiochemical mechanisms leading to DOM production for each polymer type.

2. Materials and methods

2.1 Microplastic samples

Sources. Five types of non-biodegradable microplastic samples with sizes ranging between 3–4 mm were purchased from: TOTAL, Flint Hills Resources, and Verbatim *i.e.*, PE (polyfil antistatic additive resin), PS_{col} (black plastic pellets), PE_{rec} (recycled re-grinded shreds), PP (plastic resin pellets natural injected), and PS (natural injected plastic pellets). One biodegradable microplastic was purchased from Verbatim *i.e.*, 3D printing material polylactic acid (PLA). The PLA was shipped in non-hollow filament form and was ground to 3–4 mm using a Hamilton Beach coffee grinder. Liquid nitrogen was added to prevent overheating during grinding processes. No visible changes in the microplastic morphology were noted due to liquid nitrogen addition prior to grinding.

Pre-washing process. All microplastics were washed for 2 minutes under running tap water and rinsed with distilled and deionized (DDI) water (18.2 MΩ cm) for 30 s to ensure no residual impurity was left on their surfaces. All DDI water used for cleaning and analysis was stored in glass containers to prevent plastic contamination. The amount of each polymer was left out in the open air for approximately 24 h to ensure the polymers were completely dry before experimentation. Washed and dried microplastic were placed in sealed glass containers and stored in a dark space. Photographs of each microplastic type and their respective sizes are shown in Fig. S1.† The average diameter of ten beads for each polymer type with one standard deviation is shown with the chemical formula and structure in Table 1.

2.2 Characterization of microplastic surfaces

A WITec alpha 300 R confocal Raman spectrometer was used for Raman spectroscopy. The spectrometer uses a 532 nm laser with grating at 600 g mm^{-1} and accusation time of 3 s. Raman spectroscopy was used to determine Raman intensity shifts with bond changes for both pristine and post UV aged

Table 1 Bulk surface characteristics of six polymer microplastics

Microplastic polymer	Abbreviations	Chemical formula	Molecular structure	Avg. diameter (mm) ± Std dev.	Specific surface area ($m^2\ g^{-1}$)
Polyethylene	PE	$(C_2H_4)_n$	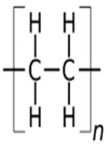	3.45 ± 0.33	7.07×10^{-3}
Polyethylene recycled	PE_{rec}	$(C_2H_4)_n$	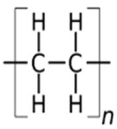	3.85 ± 0.63	4.71×10^{-3}
Polystyrene	PS	$(C_8H_8)_n$	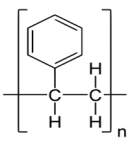	3.00 ± 0.00	9.64×10^{-3}
Polystyrene colored	PS_{col}	$(C_8H_8)_n$	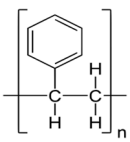	3.60 ± 0.15	3.23×10^{-3}
Polypropylene	PP	$(C_3H_6)_n$	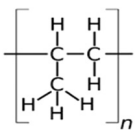	3.35 ± 0.25	1.06×10^{-2}
Polylactic acid	PLA	$(C_3H_4O_2)_n$	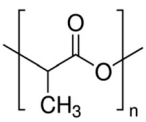	3.45 ± 0.92	8.61×10^{-3}

microplastics. FT-IR was performed using a Bruker IFS66V/S FT-IR system equipped with a mercury cadmium telluride standard detector and a KBr beam splitter with a diamond attenuated total reflectance module using a 500 nm laser. Carbonyl indices were calculated for each polymer type using the ratio of absorbance intensity of the carbonyl peak to reference peak for each polymer type. The calculation for the carbonyl indices is shown in sec. 3.2.1 A standard unpaired *t*-test was performed between pristine and aged carbonyl indices to determine if the variability was considered statistically significant (*i.e.*, *p*-value < 0.05). XPS was conducted using a VG 220i-XL equipped with a monochromated Al K-alpha X-ray source. The data analysis on the carbon and oxygen content was done using the CasaXPS software. The carbon to oxygen (C/O) ratio was calculated between pristine and post UV aged polymers to determine if the polymers were oxidizing. Surface analysis was conducted in triplicates for each method of analysis for all polymers.

The three methods of solid phase analysis provided insight into evidence of surface oxidation for each polymer type. FT-IR provided data for changing carbonyl index, RAMAN gave insight into bending and stretching of bonds due to oxidation, and XPS gave direct data on changing carbon and oxygen percentages on each polymer surface. Together, the solid phase analysis would give sufficient insights to provide the link to DOM release based on oxidizing polymers.

2.3 Microplastic aging experiments

UV irradiation experiments were completed for each of the six polymer types under identical conditions to determine DOM formation during UV aging. A photochemical aging chamber (Rayonet RPR 100) was used with 16 lamps (RPR-3500 Å) arranged in a circular pattern emitting light at ~350 nm UV-A light. UV-A light was chosen as it incorporates the most of UV spectrum from natural sunlight.[16,17] The monochromatic intensity was calculated using the formula presented in eqn (1):

$$I = \frac{P}{A} \tag{1}$$

Power was determined using the ferrioxalate actinometry method.[24] The area formulated was the area the polymers took up inside the quartz beaker. The bulbs produced 12.2 mW cm^{-2} at a distance of 12.5 cm from the center of the quartz beaker in the chamber. Over 24 h, the beads received ~0.293 kW h m^{-2} of simulated solar UV irradiance. The total solar irradiance off the coast of the southeastern United States receives ~4.87 kW h m^{-2} per day. Between 5–10% of this is UV-A, making the solar UV irradiance between 0.244–

0.487 kW h m^{-2} of simulated solar UV irradiance showing the microplastics received a similar solar UV irradiance to that in the natural environment off the coast of the southeastern United States.[25]

The experiments were conducted using 50 g of each polymer type weighed and placed in 250 mL quartz beaker with 150 mL of DDI water. 50 g was chosen as it provided a uniform dispersion of microplastic beads in the beaker allowing their access to UV light and enabled a notable organic matter release within the 24 h of UV aging time. A magnetic stir rod was added, and the beaker was placed on a stir plate inside the aging chamber. The chamber was turned on and the UV irradiation experiment was carried out for 24 h. To analyze the kinetics, 4 mL samples were taken after 1, 3, and 6 h of UV irradiation. Triplicate samples were analyzed after the completion of 24 h aging to ensure consistency of analysis techniques. PS and PE tests were run in triplicates to determine if there was statistical consistency in kinetic results for DOM formation after the 24 h. Experiments were conducted at room temperature, but due to the enclosed environment and the heat released from the UV bulbs, the DDI water was approximately 26.7 °C during the leaching experiments. The leftover solutions were poured over a Good Cook 6 inch stainless steel strainer with pore size of 0.25 mm into an amber bottle to remove aged microplastic beads from the solution. The polymers were left out to dry for 4 h and stored in a sealed glass container in the fridge after drying. A FLIR EX-Series thermal camera was used to take a thermal images at the same time intervals as the 4 mL samples were taken to ensure all bulbs were functional and emitting light uniformly for each polymer type and throughout the full 24 h. Photographs of the aging chamber and an example thermal image are shown in Fig. S2.†

Collected water samples for each polymer were analyzed *via* UV absorbance, DOC, and fluorescence through excitation emission (EEM). The analytical tools to characterize the leachate is discussed in the following section. Each polymer test was repeated with UV light off in the same chamber for 1 h stirring conditions with identical microplastic masses and DDI water volumes and compared against 1 h UV irradiation. The control experiment was conducted to capture the impact of stirring alone on leachate formation. In addition, a 1 h dark turbulent shaking experiment was set up with identical microplastic mass and DDI water volumes. In brief, 50 g of each polymer type were placed in a 250 mL amber bottle with 150 mL of DDI water. The amber bottles were secured in a sealed box and placed on a shaker and shaken at 180 rpm for 1 h. Shaking was done in a horizontal side-to-side motion. This was used to show the importance of mechanical abrasion and hydrolysis has on DOM formation for polymers in the natural environment. For dark turbulent shaking experiment, triplicates were created for each of the six polymer types. The microplastic aging experimental set-up for these dark and light conditions are summarized in Fig. S3.†

In addition, PS was tested at two other temperatures to determine how the kinetics of DOM formation might changes with increasing or decreasing temperatures. Two other temperatures of ~18.3 °C and ~35.0 °C were chosen for analysis. Temperatures were maintained using a New Brunswick Scientific C25KC incubator shaker classic series. The UV aging chamber was run inside the incubator during experimentation where thermometer readings were taken throughout experimentation to ensure consistent thermal conditions. The experiments were done in triplicates for each temperatures and samples were taken again at 1, 3, 6, and 24 h. DOC was analyzed at each time interval, where EEM was conducted after 1 and 24 h. Finally, PS DOM leachates were compared against natural organic matter (NOM) isolated from Suwannee and Mississippi Rivers obtained from International Humic Substances Society.

2.3.1 Characterization tools for microplastic leachate. To characterize the leachate formation from microplastic aging experiments, a Cary Bio 100 UV-visible spectrophotometer was used for UV absorbance measurements, using a 1 cm quartz cuvette, measuring absorbance at wavelengths from 200–800 nm. A total absorbance scan was used to monitor the amount of DOM being released during the different conditions. A Shimadzu $TOCV_{CPN}$ TOC analyzer with a Shimadzu ASI-V autosampler was used for DOC analysis. Each of the 4 mL samples were first filtered using GVS North American 0.45 μm disk membrane filters and DOC analysis was performed using the NPOC method on the $TOCV_{CPN}$. This process involved the samples being injected onto a standard TOC catalyst bed (platinum coated alumina balls) and sparged at 680 °C using ultra-pure carrier grade air. The carbon gets broken down into CO_2 and measured using a non-dispersive infrared detector (NDIR). Sample data was compared from a five-point calibration curve created using a stock solution of potassium hydrogen phthalate (KHP) purchased from Aldrich Chemical Company.

A Hitachi F-4500 fluorescence spectrophotometer was used for fluorescence analysis using emission wavelengths from 300–500 nm and excitation wavelengths from 240–400 nm. Data was processed using MATLAB R2020[a] using PARAFAC analysis techniques through drEEM toolbox to smooth the data and remove 1st and 2nd order Rayleigh and Raman scatter by using emission and excitation spectra.[26]

3. Results and discussion

3.1 DOM release

The UV aging released notable amounts of soluble organic matter from all six types of microplastics tested. Fig. 1 shows the UV spectroscopy after 1 h and 24 h UV aging and compares the data against the dark turbulent conditions and stirring control at a spectral range from 200–400 nm.

All tested polymer leachate showed an increase in UV absorbance spectra from 1 h to 24 h UV irradiation time indicating increasing DOM formation with continued UV irradiation time. The corresponding 1 h stirring (*i.e.*,

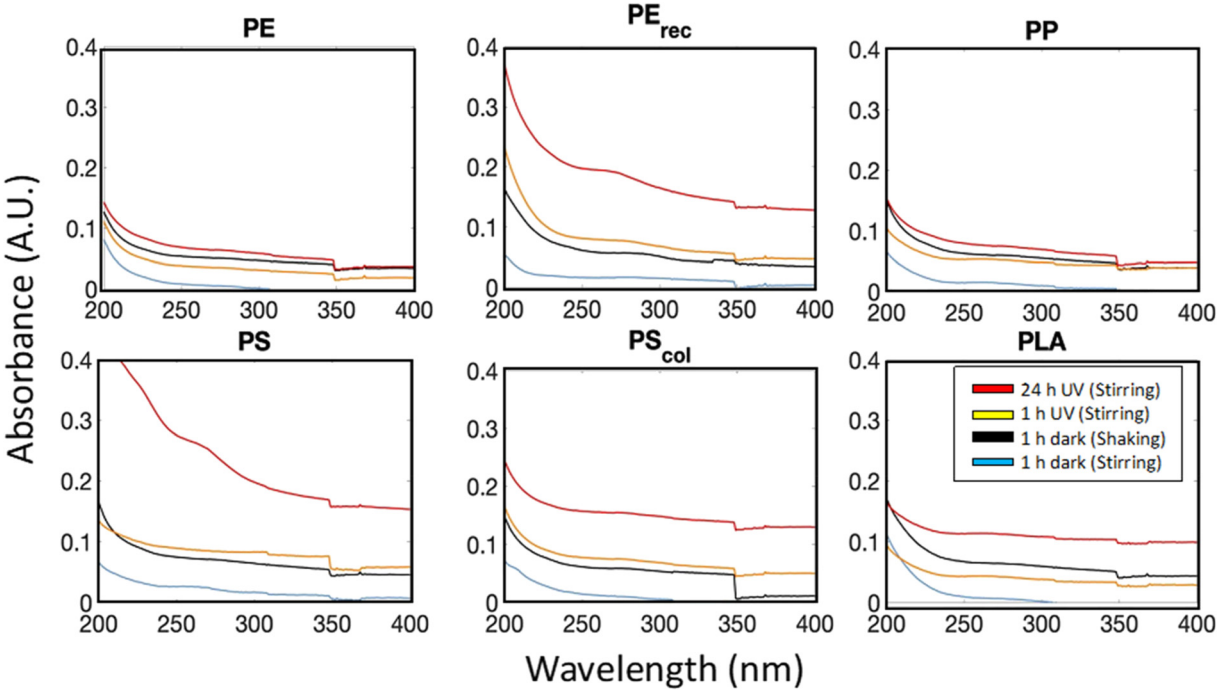

Fig. 1 UV absorbance of leachate solutions for six types of microplastics aged by 24 h and 1 h UV irradiation and associated 1 h dark controls (*i.e.*, stirring, and turbulent shaking). Absorbance values of 1 h and 24 h UV aging are arithmetic mean of triplicate experiments for PS and PE and arithmetic means of triplicate measurements of other polymers. Dark conditions and stirring control are mean of triplicate experiments for all polymers.

identical stirring with UV lamp off) showed no significant increase in UV absorbance of the leachate, resulting in liquid phase analysis results being attributed to the polymer interactions with the photons and not the stirring actions itself. The 1 h dark turbulent conditions did show relatively high absorbance, where PE, PP and PLA, 1 h dark turbulent shaking resulted in even greater DOM release when compared to 1 h UV irradiation. This indicates that UV aging is not the only factor generating leachate where mechanical abrasion and hydrolysis can be important in polymer degradation in the aquatic environment.[27]

To understand the leachate formation kinetics, UV_{254} and DOC concentrations for each polymer type were analyzed at 1, 3, 6, and 24 h (Fig. 2). Further comparison of DOC concentrations of each polymer is in Fig. S4.†

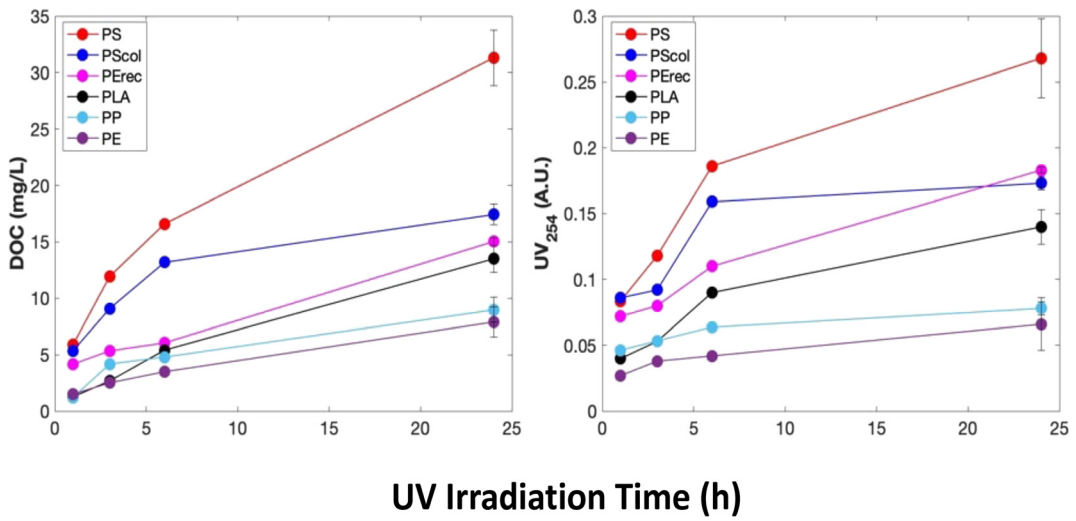

Fig. 2 UV_{254} absorbance (right) and DOC concentration in mg L^{-1} (left), for UV irradiated samples taken at 1, 3, 6, and 24 h. Error bars represent standard deviation of triplicate experiments for PE and PS, and triplicate measurements for the other polymer types. A comparison figure of UV_{254} and DOC results for each polymer after 24 h is presented in the supplementary information (Fig. S5†). Lines are drawn to guide the eye.

Consistent with UV spectral analysis, all six polymers had increasing DOC concentrations during 24 h of UV aging. The aromatic hydrocarbons, PS and PS_{col} leached the largest DOC concentrations up to 31.7 mg L^{-1} and 18.5 mg L^{-1}, respectively. The olefins leached the least, PP and PE, leaching up to 6.97 mg L^{-1} and 7.89 mg L^{-1} after 24 h irradiation. The marked differences in DOM concentration between polymer types can also be reported by normalization of mass (in mg) of DOC release per mass (in grams) of microplastic. One gram of microplastic in the UV aging chamber released the following amounts of DOC (in mg) over 24 h: PS (0.10) > PS_{col} (0.06) > PE_{rec} (0.05) > PLA (0.04) > PP (0.03) > PE (0.02). These values are minute (<0.01 wt%) in comparison to the total mass of microplastic in the aging chamber over the 24 h indicating the potential for long term DOC release during their retention in the environment. Similarly, the DOM concentration can be normalized against the surface area of each polymer type, where 1 m^2 of MP leached the following masses of DOC (in mg) over 24 h: PS (9.9), PS_{col} (17), PE_{rec} (9.6), PLA (4.7), PP (2.5), PE (3.4). The order of DOC release is similar between surface area and mass normalization between polymer types, but PS_{col} had the highest potential of release per m^2. It should be noted that the release takes place from the surface of MPs and the larger surface area is, the more mass they can release under UV irradiation.[21]

3.1.1 Characterization of dissolved organic matter by fluorescence spectroscopy. To characterize the DOM from these polymers, fluorescence was measured using excitation (240–400 nm) and emission (300–460 nm) to characterize the leachate based on the sector that fluoresces (Fig. 3).[28] Fluorescence is measured in intensity, a unitless value measured in arbitrary units (a.u.) that is directly proportional to concentration with increasing intensity, coinciding with increasing DOM concentration. A comparison of the matrix of each polymer type after 1 h and 24 h UV irradiation is shown in Fig. 3.

Intensity is represented by intensity peaks, the highest value of the matrix resembling a mountain peak. The intensity peaks of EEM increased in all six polymers from 1 to 24 h UV aging, which aligns with the UV absorbance and DOC results. PS showed the largest intensity peak increase (143 → 237 a.u.) followed by PS_{col} (100 → 182 a.u.). The sector the organic matter that is fluorescing for the PS polymers is within the aromatic sector, showing the organic matter being released from the surface is not just aromatic impurities, but organic matter from the polymer itself may be released. PE_{rec} also had a larger increase in peak intensity (248 → 329 a.u.) and fluoresced within the aromatic sector. This most likely is attributed to the introduction of polycyclic aromatic hydrocarbons (PAHs) during the production process. Phenanthrene is a common compound introduced

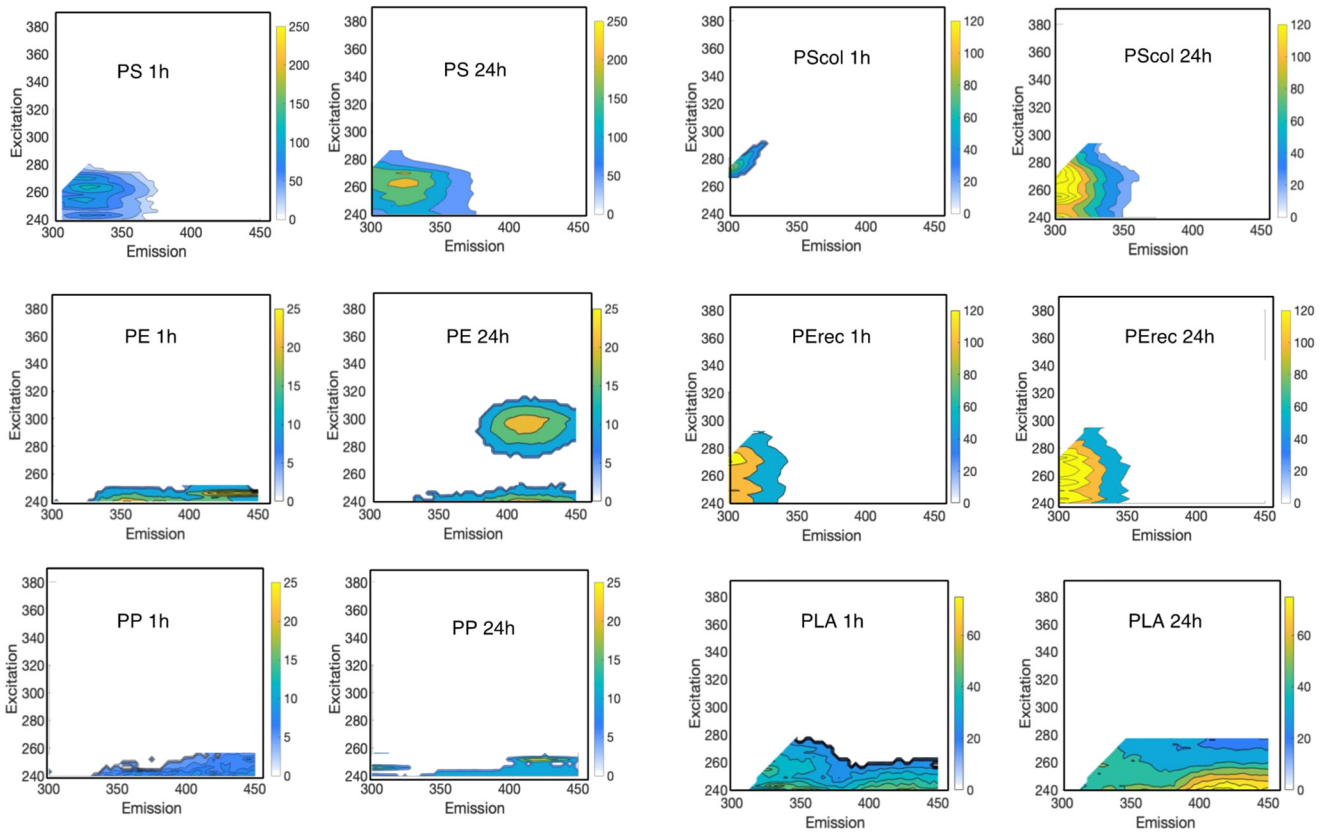

Fig. 3 Fluorescence analysis using excitation (240–400 nm) and emission (300–450 nm) after 1 h UV irradiation and 24 h UV irradiation. 24 h intensity values are arithmetic mean of triplicate experiments for PS and PE and arithmetic means of triplicate measurements of other polymers.

and can be easily adsorbed to the microplastic surfaces during remolding.[29] The aliphatic polymers, PP (9.69 → 24.7 a.u.) and PE (25.9 → 34.8 a.u.) showed very small peak intensity increases in the fulvic and humic acid sectors which makes it difficult to determine whether organic matter was coming off these polymer surfaces. The lower DOC concentrations for PE and PP combined with the EEM intensities shows that the organic material may be impurities released from the polymer chain and not directly organic material. The highest intensity increases for an aliphatic for PLA (55.2 → 97.0 a.u.) coincided well with the larger DOC concentration after 24 h (13.5 mg L^{-1}), which may be explained by its greater biodegradability. There was consistency between each mode of liquid phase analysis where it was clear that PS was leaching off a significant increase of DOM compared to PP and PE.

3.1.2 Photooxidation pathways. During UV irradiation, all polymers undergo three major processes: initiation, propagation, and termination. Initiation is the creation of free radical carbons ($R^{\bullet}$) due to photons being absorbed by chemical bonds. Most polymers are photo-inert to wavelengths >290 nm, meaning initiation from UV-A light must stem from impurities attached to the polymer chain. The ability of a polymer to generate free radical carbons can vary greatly depending on the chemical structure, impurities bonded to the polymer chain, and surface area exposed to photons. Also, the mechanisms of generating free radical carbons are similar and the variation between an aromatic and aliphatic polymer likely lead to the significant differences in DOM formation over 24 h. PS has a phenyl ring with delocalized π bonds along the outside making free radical generation rapid compared to a straight chain polymer such as PE and PP.[30] Free radical generation can be represented as a spherical ball on a hill. Once it gets started it will autonomously react, so with PS generating free radical carbons faster it increased the rate of DOM formation.

The second step of photooxidation is propagation. As free radicals are generated, they begin to combine with oxygen where hydrogen abstraction occurs. A hydrogen atom gets removed from the polymer chain, creating hydroperoxide (ROOH). These are intermediates, which can absorb UV irradiation 300–500× greater than a pure polymer.[3] Alkoxyl and hydroxyl radicals form and the polymer chain begins to propagate. Cross-linking occurs where the polymer chains bond together, which significantly weakens a polymer surface and makes it susceptible to fragmentation and surface cracking. Ketones can be introduced during oxidation where a Norrish II reaction occurs and C–C bonds can break, causing the chain scission of the polymer backbone.[31–33] Initiation and propagation steps are shown in eqn (2)–(4).

$$\text{Polymer} \rightarrow R^{\bullet} \quad (2)$$

$$R^{*} + O_2 \rightarrow ROO^{\bullet} \quad (3)$$

$$ROO^{\bullet} + H \rightarrow ROOH + R^{\bullet} \quad (4)$$

In our analysis PE leached higher DOM concentration than PP, but longer-term studies have shown PP to leach larger DOM concentrations *versus* PE due to these alkyl groups on the PP polymer chain are more likely to cause chain scission over time.[23,33] PE_{rec} leached 15 mg L^{-1} compared to the pristine PE of 8 mg L^{-1} after 24 h. This is most likely attributed to the introduction of the PAHs as seen during EEM analysis. The introduction of PAHs helps to generate free radical carbons at faster rates due to similar processes of that seen for PS allowing for higher DOM formation. The rapid formation of hydroperoxides and hydroxyl radicals for PS for longer term studies have been shown to inhibit further aging due to the rapid production of these intermediates.[13]

The thermal images allowed for insurance that each polymer was receiving similar amounts of photons over the course of the 24 h UV irradiation. As a result, the chemical structure is essential in the kinetic rate and mass of DOM formation. A polymer that can rapidly generate free radical carbons will increase the rate of DOM leaching from the polymer surface. Evidence of this variation is seen throughout each mode of liquid phase analysis, where PS showed greater EEM intensity, DOC concentration, and UV absorbance over the 24 h compared to the other polymers.

3.1.3 Effect of temperature on DOM formation. All MP types were shown to be leaching organic matter and how temperature affects leachate formation was further explored to reveal some mechanistic insights on leachate formation. PS was chosen for temperature comparison as it showed highest UV absorption, DOC concentration and fluorescence intensity peak increase. Initial experiments with PS were conducted at ~26.7 °C. To create a temperature comparison, two more environmentally relevant temperatures were chosen at 18.3 °C and 35.0 °C. Experiments were carried out in triplicates with 4 mL samples were taken at 1, 3, 6, and 24 h. The resulting DOC concentrations are presented in Fig. 4.

The results show that leachate formation depends on the ambient temperature. Decreasing the temperature to 18.3 °C

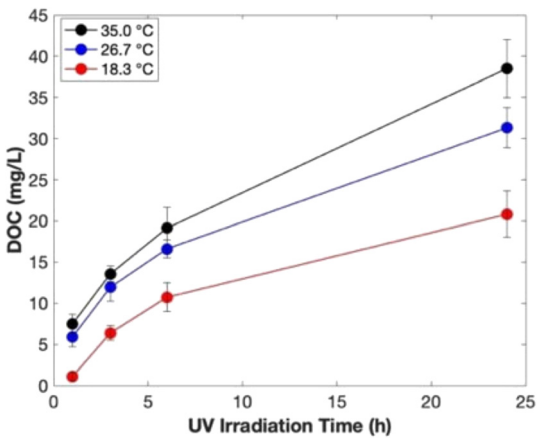

Fig. 4 DOC formation kinetics comparison of PS at 35.0, 26.7 and 18.3 °C after 24 h irradiation. Error bars represent one standard deviation of triplicate experiments for each temperature.

reduced the DOC concentration from 32 to 20 mg L^{-1}. Increasing the temperature to 35.0 °C resulted in DOC concentrations increasing from 32 to 37 mg L^{-1}. This indicates that microplastics in warmer environments will degrade faster.[3] The temperature comparison of PS shows the importance of the initiation step during photooxidation where increasing temperatures can help to initiate photooxidation. To analyze the kinetics further, the kinetic leachate formation constants (k_T) were calculated fitting the formation data to zero order reactions for each temperature used as: $k_{18.3}$ = 0.84 mg L^{-1} h^{-1}, $k_{26.7}$ = 1.06 mg L^{-1} h^{-1}, and $k_{35.0}$ = 1.26 mg L^{-1} h^{-1}. The rate constants were plotted against $1/T$ using the Arrhenius equation (eqn (5)).

$$k = A\frac{-E_A}{RT} \quad (5)$$

and the resulting slope was the minimum activation energy over the real gas constant $\left(\frac{E_A}{R}\right)$. The minimum energy required for the formation of PS leachate to occur was +18.3 kJ mol^{-1} aligning well with the previous reports.[34] To further show the impact of temperature, the EEM results complemented the DOC results as shown in Fig. 5. Peak intensities diminished at the lower temperatures after 24 h (237 → 94.1 a.u.) and increased at the higher temperatures (237 → 387 a.u.). MPs such as PS would degrade at different rates depending on the temperature; however, other MP types may need to be evaluated to make a conclusive statement about the overall leachate formation.

3.2 Characterization of pristine and aged microplastic surfaces

3.2.1 Raman and Fourier transform spectroscopy. Raman spectroscopy (Fig. S5†) and FT-IR (Fig. 6) were performed on all six polymers to compare the pristine and post 24 h UV aged surface characteristics. Raman spectroscopy shows relative frequencies to distinguish between molecular bond changes, FT-IR shows absolute frequencies of radiation absorbance to determine functional group vibrations and polar bonds. Each can analyze surface oxidation by the formation of hydroxyl, carboxyl, and carbonyl groups.[20] Raman spectroscopy was performed on all six polymers using a 532 nm laser. Two dyed polymers did not have clear signals during Raman spectroscopy analysis.[35] However, the four white polymers (PE, PS, PLA, and PP) presented clear Raman spectral data (Fig. S5†).

The characteristic peaks with decreasing intensity between 1 and 24 h are present for each polymer, PS at 1000 cm^{-1}, PP at 695 cm^{-1}, and PE at 1059 cm^{-1}, presenting evidence for UV aging.[36] On the other hand, PLA was tested thrice, and the Raman results remained scattered. The scattering may be attributed to the molecular stability of the PLA.[36] The methyl, methylene and methine peaks at wavenumber of 2800–3000 cm^{-1} for all four microplastics becomes attenuated with aging, signaled through CH_2 and CH stretching. The CH_2 bending from 1400–1450 cm^{-1} for PS and peak from 1680–1800 cm^{-1} for PLA signifies that PS and PLA formed aldehydes from the formation of a carbonyl group post UV aging.[37] This occurs due to free radicals causing the chain scission of the C–H bonds of PLA and PS. The symmetry at

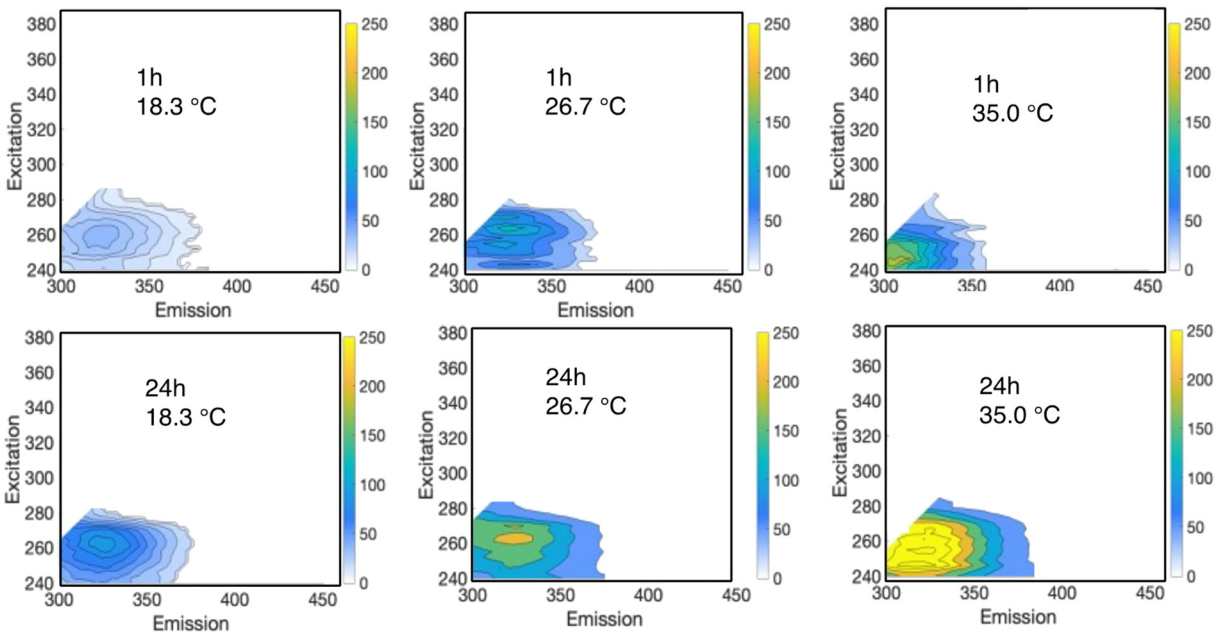

Fig. 5 EEM comparison of PS at 35.0, 26.7 and 18.3 °C after 1 h (top) and 24 h (bottom) irradiation. It should be noted that different temperature graphs have different intensity ranges to pronounce the changes in EEM. Intensity is arithmetic mean of triplicates for each temperature and at each time interval.

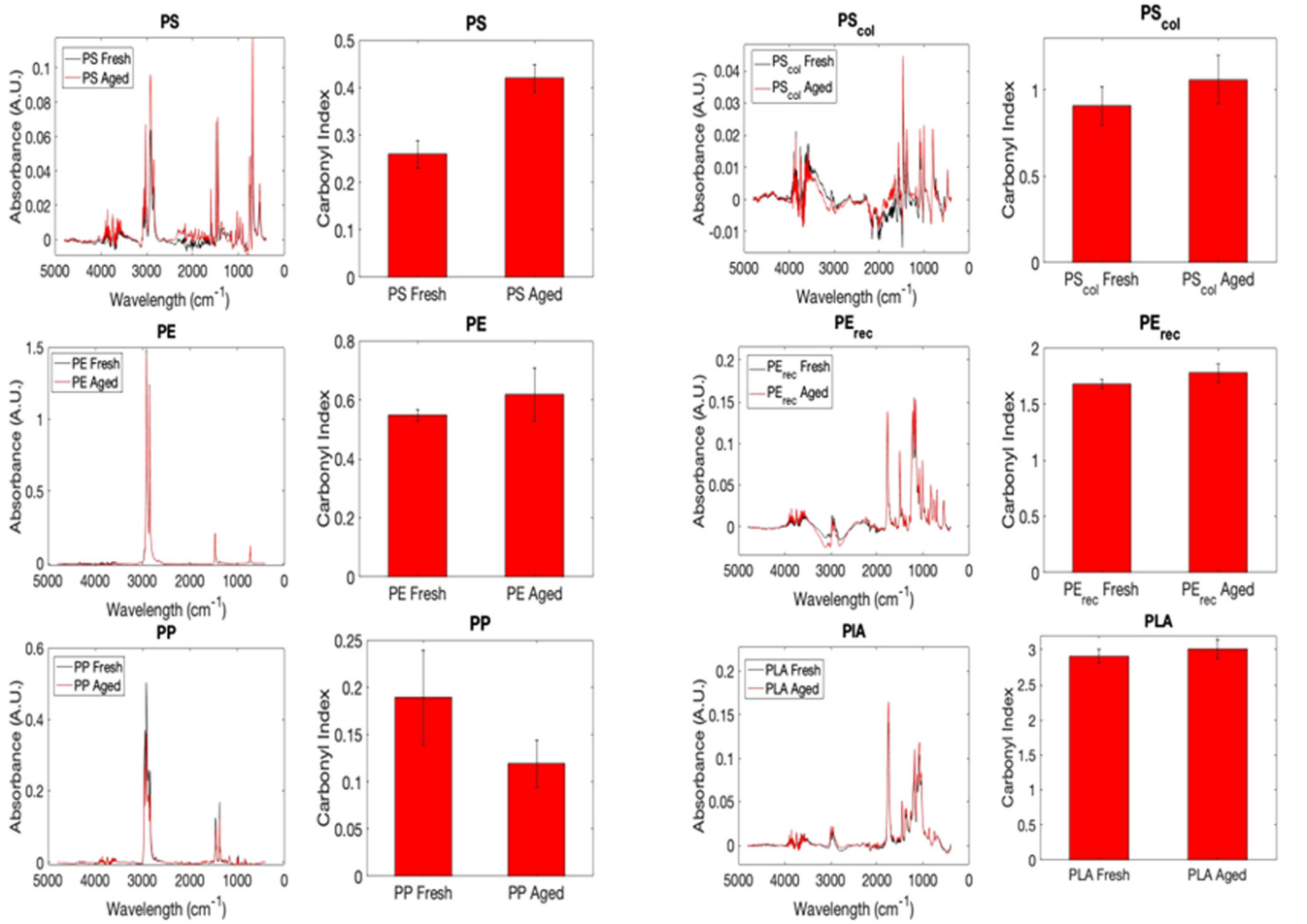

Fig. 6 FT-IR absorbance from 4000–1000 cm^{-1} (left). Calculated carbonyl indices with one standard deviation error bars (right). Spectrums are arithmetic mean values of triplicates for each polymer type.

1600 cm^{-1} signifies that PP and PE followed similar hydroperoxide formation, however, resulted in alkene formation post UV aging.[38]

For each polymer, the Raman results presented evidence of surface oxidation.

FT-IR was performed to determine carbonyl indices for each polymer type from pristine to post UV aged. FT-IR spectrums and corresponding carbonyl indices for all microplastics are presented in Fig. 6. The carbonyl index was calculated from FT-IR by dividing the carbonyl peak absorbance to reference peak absorbance for each polymer. Each carbonyl and reference peak was determined based on literature *i.e.*, $\mathrm{PE}\left(\frac{1716\ cm^{-1}}{1375\ cm^{-1}}\right)$, $\mathrm{PS}\left(\frac{1720\ cm^{-1}}{1450\ cm^{-1}}\right)$, $\mathrm{PLA}\left(\frac{1748\ cm^{-1}}{1451\ cm^{-1}}\right)$ and $\mathrm{PP}\left(\frac{1712\ cm^{-1}}{1456\ cm^{-1}}\right)$.[39–41]

Carbonyl index increased in all polymers, but PP. PS was the only statistically significant increase (p-value < 0.05) after the 24 h UV aging. The increasing carbonyl index of PS (0.26–0.42) and PS_{col} (0.91–1.07) is due to these polymers being favorable to aging seen through DOM formation analysis, FT-IR and Raman results.[42,43] There were also characteristic peaks at 1470 cm^{-1} and 720 cm^{-1} for each polymer associated with the C–H bending of CH_2 bonds showing UV aging.[44] Increasing number of peaks also can signify formation of functional groups, where for all six polymers, there were an increasing number of peaks from 1780–1684 cm^{-1} showing the formation of oxygen containing functional groups such as a carbonyl group, ester formation, or γ-lactones.[45]

3.2.2 X-ray photoelectron spectroscopy. In all microplastics, there were clear evidence regarding the oxidation of surfaces. Some microplastics with aromatic monomers, *e.g.*, PS and

Table 2 Carbon and oxygen content with carbon to oxygen ratio

Sample	C (%)	O (%)	C/O
PE fresh	98.4	1.63	60.4
PE aged	78.0	2.78	28.1
PP fresh	99.0	0.99	99.0
PP aged	51.4	4.61	11.1
PLA fresh	46.1	32.6	1.41
PLA aged	41.6	48.0	0.867
PS fresh	94.6	5.41	17.5
PS aged	92.9	7.10	13.1
Recycled PE fresh	74.5	23.5	3.17
Recycled PE aged	45.2	16.2	2.79
Colored PS fresh	62.7	10.4	6.03
Colored PS aged	59.5	14.4	4.13

PS_{col}, were oxidizing more than the aliphatic ones *e.g.*, PP. To further quantify the surface oxidation of each polymer pre- and post-aging, XPS wide scanning was also conducted, and carbon and oxygen content was quantified. It is a surface sensitive method to analyze elemental percentage on the surface of each microplastics as shown in Table 2.

Two important trends to highlight is the oxidation of a polymer during UV aging processes through XPS, is increasing oxygen percent and decreasing C/O ratio as surface oxidation occurs. For all six polymers there was increasing oxygen content through surface oxidation and decreasing C/O ratio. XPS results differed from FT-IR as PP showed the largest decrease in C/O ratio showing (80%) followed by PE (54%) and PS_{col} (32%). The two largest reductions in C/O ratio were from aliphatic hydrocarbons. The remaining percentages of composition can be attributed to fluorine and neon. Many plastics are fluorinated with fluorine gas to create a surface barrier.[46] The introduced neon could best be assumed to occur through the UV-A bulbs, where neon is introduced for germicidal purposes and may leak out over time.[46] Neon has been found to bond to hydrogen fluoride over time and is the best estimation for why neon and fluorine were seen for polymers during XPS analysis.[47] PLA had a low starting carbon content but is consistent with values presented within the literature due to the impurities introduced during manufacturing processes.[48–50] The XPS results show significant surface oxidation, much higher than the results presented in RAMAN and FT-IR analysis, but the essential factor is the C/O ratio was decreasing for all six polymers, signifying that DOM formation was the result of surface oxidation and not just impurities degrading from the polymer chain that the EEM results might have suggested.

3.3 Implications on water quality

The results of this study indicate the link between surface oxidation and DOM leaching from microplastics. Microplastic-based DOM release poses possible harm to drinking water sources. Many facilities are designed to remove NOM from water but are not necessarily equipped for handling higher aromatic leachate removal as most NOM is comprised of humic and fulvic acids. This difference is demonstrated with EEM comparison of PS leachate, Mississippi River NOM, and Suwannee River NOM at 32 mg L^{-1} (Fig. 7). The peak locations as well as overall intensities of fluorescence signals are different between NOM and PS leachate at the same DOC concentrations.

The inherent difference between the DOM makeup combined with the excessively large surface area of microplastisphere, is an overwhelming new anthropogenic domain that may change the dissolved organic matter concentration in the environment especially in locations where MPs prevail. The UV irradiation could accelerate the leachate formation and further threaten the ecological health with a potential burden to existing water treatment infrastructure that is dating back to the Victorian era. Even with modern water treatment technologies that are using membrane removal methods with polymeric materials such as polyvinylidene fluoride (PVDF) has found MPs in their effluents.[51] This is also true for other plastic-based water treatment methods including nanofiltration and reverse osmosis.[52] The removal potential and methodology used for different polymer types is still a new domain for water treatment. Each leachate type may require new strategies for removal and ways to handle increasing sludge production. PS leached DOM at a significantly higher rate than the other polymers and just the shear amount of DOM reaching water treatment presents its own challenges. Lastly, the chemical transformation potential, reactivity under disinfection conditions and sheer toxicity of MPs leachate deems further research.

Conclusions

This study analyzed six different polymer types of microplastics undergoing 24 h UV irradiation. The work attempts to create a compound analysis that MP surface analysis techniques of XPS, FT-IR and Raman Spectroscopy are coupled with DOM analysis after the 24 h to create a link between surface oxidation and leachate production. The results suggest that aromatic polymers oxidize and release DOM much more rapidly from UV irradiation compared to aliphatic ones. The surface and DOM results were consistent for each mode of analysis that PS had the highest DOM concentration and surface oxidation. This can most likely be attributed to the phenyl ring introducing free radicals at much faster rates than that of a straight chain polymer. The

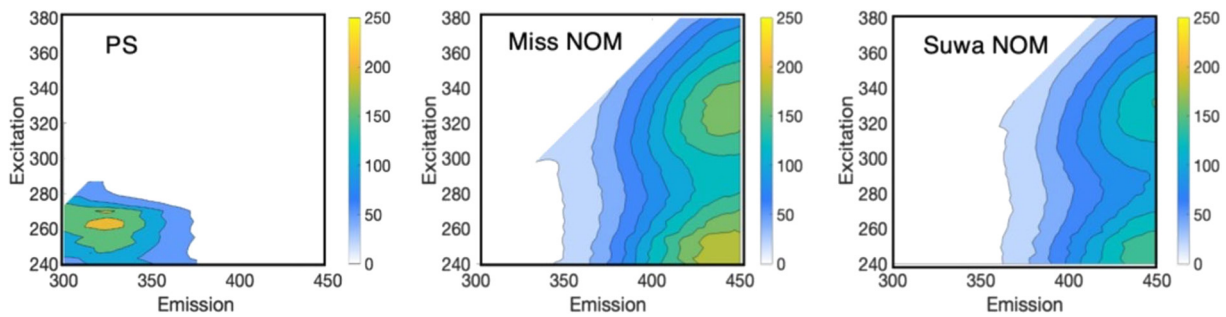

Fig. 7 EEM comparison of PS and DOM from Suwanee and Mississippi Rivers. All samples have a DOC concentration of 32 mg L^{-1}. Intensity values are triplicates for each NOM samples and PS.

temperature comparison of PS provides further evidence of the importance of the initiation step during photooxidation where increasing temperatures can help to initiate photooxidation faster seen by the increasing kinetic rate and mass of DOM formation of PS with increasing temperatures. The temperature analysis also indicated the endothermic nature of DOM release from PS MPs by determining the activation energy required to initiate photooxidation. PS degrades at faster rates than aliphatic polymers, but they all provide their own issues to marine organisms and water quality. All MP pollution is environmentally detrimental, and these results suggest DOM release from polymers may persist within the environment and requires attention by policymakers, researchers, and the practitioners.

Conflicts of interest

There is no competing financial interest between authors.

Disclaimer

The research presented was not performed or funded by EPA and was not subject to EPA's quality system requirements. The views expressed in this article are those of the author(s) and do not necessarily represent the views or the policies of the U.S. Environmental Protection Agency.

Acknowledgements

This work was financially supported by National Science Foundation through ECS 2003859 and ECS 2004160 awards. The manuscript has not been subjected to the peer and policy review of the agency and does not necessarily reflect their views.

References

1 R. Geyer, J. R. Jambeck and K. L. Law, Production, use, and fate of all plastics ever made, *Sci. Adv.*, 2017, **3**, 1–12.
2 M. Eriksen, L. C. M. Lebreton, H. S. Carson, M. Thiel, C. J. Moore, J. C. Borerro, F. Galgani, P. G. Ryan and J. Reisser, Plastic pollution in the world's oceans: More than 5 trillion plastic pieces weighing over 250,000 tons afloat at sea, *PLoS One*, 2014, **9**, 1–15.
3 D. Feldman, Polymer weathering: photo-oxidation, *J. Polym. Environ.*, 2002, **10**, 163–173.
4 R. C. Thompson, Y. Olsen, R. P. Mitchell, A. Davis, S. J. Rowland, A. W. G. John, D. McGonigle and A. E. Russell, Lost at sea Where is all the plastic?, *Science*, 2004, **304**, 838.
5 J. Zhou, H. Gui, C. C. Banfield, Y. Wen, H. Zang, M. A. Dippold, A. Charlton and D. L. Jones, The microplastisphere: biodegradable microplastics addition alters soil microbial community structure and function, *Soil Biol. Biochem.*, 2021, **156**, 108211.
6 M. Ateia, G. Ersan, M. G. Alalm, D. C. Boffito and T. Karanfil, Emerging investigator series: microplastic sources, fate, toxicity, detection, and interactions with micropollutants in aquatic ecosystems – a review of reviews, *Environ. Sci.: Processes Impacts*, 2022, **24**, 172–195.
7 E. Costigan, A. Collins, M. D. Hatinoglu, K. Bhagat, J. Macrae, F. Perreault and O. Apul, Adsorption of organic pollutants by microplastics: Overview of a dissonant literature, *J. Hazard. Mater. Adv.*, 2022, **6**, 100091.
8 S. Lambert and M. Wagner, Characterization of nanoplastics during the degradation of polystyrene, *Chemosphere*, 2016, **145**, 265–268.
9 Y. K. Lee and J. Hur, Adsorption of microplastic-derived organic matter onto minerals, *Water Res.*, 2020, **187**, 116426.
10 M. Ateia, A. Kanan and T. Karanfil, Microplastics release precursors of chlorinated and brominated disinfection byproducts in water, *Chemosphere*, 2020, **251**, 126452.
11 M. M. Mortula, S. Atabay, K. P. Fattah and A. Madbuly, Leachability of microplastic from different plastic materials, *J. Environ. Manage.*, 2021, **294**, 112995.
12 J. Brandon, M. Goldstein and M. D. Ohman, Long-term aging and degradation of microplastic particles: comparing in situ oceanic and experimental weathering patterns, *Mar. Pollut. Bull.*, 2016, **110**, 299–308.
13 K. Zhu, H. Jia, Y. Sun, Y. Dai, C. Zhang, X. Guo, T. Wang and L. Zhu, Long-term phototransformation of microplastics under simulated sunlight irradiation in aquatic environments: Roles of reactive oxygen species, *Water Res.*, 2020, **173**, 115564.
14 T. P. Coohill and J. L. Sagripanti, Bacterial inactivation by solar ultraviolet radiation compared with sensitivity to 254 nm radiation, *Photochem. Photobiol.*, 2009, **85**, 1043–1052.
15 A. L. Santos, V. Oliveira, I. Baptista, I. Henriques, N. C. M. Gomes, A. Almeida, A. Correia and Â. Cunha, Wavelength dependence of biological damage induced by uv radiation on bacteria, *Arch. Microbiol.*, 2013, **195**, 63–74.
16 J. D'Orazio, S. Jarrett, A. Amaro-Ortiz and T. Scott, UV radiation and the skin, *Int. J. Mol. Sci.*, 2013, **14**, 12222–12248.
17 A. Müller, R. Becker, U. Dorgerloh, F. G. Simon and U. Braun, The effect of polymer aging on the uptake of fuel aromatics and ethers by microplastics, *Environ. Pollut.*, 2018, **240**, 639–646.
18 L. Cai, J. Wang, J. Peng, Z. Wu and X. Tan, Observation of the degradation of three types of plastic pellets exposed to UV irradiation in three different environments, *Sci. Total Environ.*, 2018, **628**, 740–747.
19 P. Liu, Y. Shi, X. Wu, H. Wang, H. Huang, X. Guo and S. Gao, Review of the artificially-accelerated aging technology and ecological risk of microplastics, *Sci. Total Environ.*, 2021, **768**, 144969.
20 R. Mao, M. Lang, X. Yu, R. Wu, X. Yang and X. Guo, Aging mechanism of microplastics with UV irradiation and its effects on the adsorption of heavy metals, *J. Hazard. Mater.*, 2020, **393**, 122515.
21 C. Wang, Z. Xian, X. Jin, S. Liang, Z. Chen, B. Pan, B. Wu, Y. S. Ok and C. Gu, Photo-aging of polyvinyl chloride microplastic in the presence of natural organic acids, *Water Res.*, 2020, **183**, 116082.

22 K. Bhagat, A. C. Barrios, K. Rajwade, A. Kumar, J. Oswald, O. Apul and F. Perreault, Aging of microplastics increases their adsorption affinity towards organic contaminants, *Chemosphere*, 2022, **298**, 134238.

23 Y. K. Lee, C. Romera-Castillo, S. Hong and J. Hur, Characteristics of microplastic polymer-derived dissolved organic matter and its potential as a disinfection byproduct precursor, *Water Res.*, 2020, **175**, 115678.

24 R. E. Kalan, S. Yaparatne, A. Amirbahman and C. P. Tripp, P25 titanium dioxide coated magnetic particles: Preparation, characterization and photocatalytic activity, *Appl. Catal., B*, 2016, **187**, 249–258.

25 ESMAP, *Global Photovoltaic Power Potential by Country*, World Bank, Washington, DC, 2020.

26 K. R. Murphy, C. A. Stedmon, D. Graeber and R. Bro, Fluorescence spectroscopy and multi-way techniques PARAFAC, *Anal. Methods*, 2013, **5**, 6557–6566.

27 W. Chen, P. Westerhoff, J. A. Leenheer and K. Booksh, Fluorescence excitation-emission matrix regional integration to quantify spectra for dissolved organic matter, *Environ. Sci. Technol.*, 2003, **37**, 5701–5710.

28 A. Alassali, W. Calmano, E. Gidarakos and K. Kuchta, The degree and source of plastic recyclates contamination with polycyclic aromatic hydrocarbons, *RSC Adv.*, 2020, **10**, 44989–44996.

29 E. Yousif and R. Haddad, Photodegradation and photostabilization of polymers, especially polystyrene: review, *Springerplus*, 2013, **2**, 1–32.

30 P. Gijsman and J. Sampers, The influence of oxygen pressure and temperature on the uv-degradation chemistry of polyethylene, *Polym. Degrad. Stab.*, 1997, **58**, 55–59.

31 M. Gardette, S. Thérias, J. L. Gardette, M. Murariu and P. Dubois, Photooxidation of polylactide/calcium sulphate composites, *Polym. Degrad. Stab.*, 2011, **96**, 616–623.

32 S. Bocchini and A. Frache, Comparative study of filler influence on polylactide photooxidation, *eXPRESS Polym. Lett.*, 2013, **7**, 431–442.

33 S. Aslanzadeh and M. H. Kish, Photo-oxidation of polypropylene fibers exposed to short wavelength UV radiations, *Fibers Polym.*, 2010, **11**, 710–718.

34 C. P. Ward, C. J. Armstrong, A. N. Walsh, J. H. Jackson and C. M. Reddy, Sunlight converts polystyrene to carbon dioxide and dissolved organic carbon, *Environ. Sci. Technol. Lett.*, 2019, **6**, 669–674.

35 D. Saviello, M. Trabace, A. Alyami, A. Mirabile, P. Baglioni, R. Giorgi and D. Iacopino, Raman spectroscopy and surface enhanced Raman scattering (SERS) for the analysis of blue and black writing inks: Identification of dye content and degradation processes, *Front. Chem.*, 2019, **7**, 1–9.

36 Z. Sobhani, M. Al Amin, R. Naidu, M. Megharaj and C. Fang, Identification and visualization of microplastics by Raman mapping, *Anal. Chim. Acta*, 2019, **1077**, 191–199.

37 A. Araújo, G. B. Botelho, M. Silva and A. V. Machado, UV stability of poly(lactic acid) nanocomposites, *J. Mater. Sci. Eng. B*, 2013, **3**, 75–83.

38 T. Hüffer, A. K. Weniger and T. Hofmann, Sorption of organic compounds by aged polystyrene microplastic particles, *Environ. Pollut.*, 2018, **236**, 218–225.

39 M. Dong, Q. Zhang, X. Xing, W. Chen, Z. She and Z. Luo, Raman spectra and surface changes of microplastics weathered under natural environments, *Sci. Total Environ.*, 2020, **739**, 139990.

40 C. Rouillon, P. O. Bussiere, E. Desnoux, S. Collin, C. Vial, S. Therias and J. L. Gardette, Is carbonyl index a quantitative probe to monitor polypropylene photodegradation?, *Polym. Degrad. Stab.*, 2016, **128**, 200–208.

41 E. Yousif, J. Salimon and N. Salih, New stabilizers for polystyrene based on 2-Nsalicylidene-5-(substituted)-1,3,4-thiadiazole compounds, *J. Saudi Chem. Soc.*, 2012, **16**, 299–306.

42 E. S. Medeiros, J. E. Oliveira, M. Rego, M. Rego and C. Branco, Soil biodegradation of PLA/CNW nanocomposites modified with ethylene oxide derivatives, *Mater. Res.*, 2018, **2**, 1–6.

43 N. A. Weir and K. Whiting, Initial steps in the photolysis and photooxidation of polystyrene, *Eur. Polym. J.*, 1989, **25**, 291–295.

44 G. Geuskens, D. Baeyens-Volant, G. Delaunois, Q. Lu-Vinh, W. Piret and C. David, Photo-oxidation of polymers-I. A quantitative study of the chemical reactions resulting from irradiation of polystyrene at 253.7 nm in the presence of oxygen, *Eur. Polym. J.*, 1978, **14**, 291–297.

45 A. Benítez, J. J. Sánchez, M. L. Arnal, A. J. Müller, O. Rodríguez and G. Morales, Abiotic degradation of LDPE and LLDPE formulated with a pro-oxidant additive, *Polym. Degrad. Stab.*, 2013, **98**, 490–501.

46 G. Kranz, R. Lüschen, T. Gesang, V. Schlett, O. D. Hennemann and W. D. Stohrer, The effect of fluorination on the surface characteristics and adhesive properties of polyethylene and polypropylene, *Int. J. Adhes. Adhes.*, 1994, **14**, 243–253.

47 M. Losonczy, J. W. Moskowitz and F. H. Stillinger, Hydrogen bonding between neon and hydrogen fluoride, *J. Chem. Phys.*, 1974, **61**, 2438–2441.

48 Z. A. Abdul Hamid, C. Y. Tham and Z. Ahmad, Preparation and optimization of surface- engineered poly(lactic acid) microspheres as a drug delivery device, *J. Mater. Sci.*, 2018, **53**, 4745–4758.

49 I. Lednev, E. Salomatina, S. Ilyina, S. Zaitsev, R. Kovylin and L. Smirnova, Development of biodegradable polymer blends based on chitosan and polylactide and study of their properties, *Materials*, 2021, **14**, 1–17.

50 C. Boonmee, C. Kositanont and T. Leejarkpai, Degradation of poly (lactic acid) under simulated landfill conditions, *Environ. Nat. Resour. J.*, 2016, **14**, 1–9.

51 J. Sun, Z. R. Zhu, W. H. Li, X. Yan, L. K. Wang, L. Zhang, J. Jin, X. Dai and B. J. Ni, Revisiting microplastics in landfill leachate: unnoticed tiny microplastics and their fate in treatment works, *Water Res.*, 2021, **190**, 1–11.

52 Z. Zhang, Y. Su, J. Zhu, J. Shi, H. Huang and B. Xie, Distribution and removal characteristics of microplastics in different processes of the leachate treatment system, *Waste Manage.*, 2021, **120**, 240–247.

